Vol. 45, No. 4 (2023) 710-717, DOI: 10.24874/ti.1524.07.23.08

Tribology in Industry

www.tribology.rs

RESEARCH

Effective Strains Determination in Continuous Constrained Double Bending with Active Friction Forces

Valentin Kamburov[a,*] and Antonio Nikolov[a]

[a]*Department of Materials Science and Technology, Faculty of Industrial Tecnology, Technical University of Sofia, Bulgaria.*

Keywords:

Severe plastic deformation
Constrained continuous double bending
ECAE conform process
CAD/CAE software 3D simulation

* Corresponding author:

Valentin Kamburov
E-mail: vvk@tu-sofia.bg

Received: 20 July 2023
Revised: 14 August 2023
Accepted: 15 September 2023

A B S T R A C T

In this work, a new process for severe plastic deformation (SPD) with active friction forces - CCDB Conform R3D2, a variation of the so-called "active bending", which is a continuous two-stage bending in calibers with small relative bending radius, is analyzed. A mechanical scheme of a device for realization of the process with a bending roller is proposed, based on a developed 3D virtual tool for its realization. Using CAD/CAE software 3D simulation, two virtual solutions of the process were compared, differing in terms of the location of the bending roller relative to the axes of the feeding and output rolls. The distribution and magnitude of the effective strains in the volume of the deformed long workpiece in the two bending stages at small relative bending radiuses were analyzed. An analytical expression is developed to determine the effective strains achieved in the SPD operation by constrained continuous bending in calibers with grooved rolls. The strain calculation methodology is based on the results obtained by simulation modelling of the CCB Conform R3D2 process in trapezoidal calibers with a bending roller located above and below the rolls line.

1. INTRODUCTION

In order to realize severe plastic deformation (SPD) in practice, mechanical deformation schemes with three-dimensional compressive stresses, a closed or highly constrained deformation space and a concentrated deformation zone of simple/pure shear are used [1,2]. Technological operations for SPD are divided into several groups according to the ratio of the volume of the deformed to the volume of the non-deformed zone of the workpiece and the number of passes for which the original shape of the non-deformed billet is restored [1-3].

In the severe plastic deformation group of operations with active friction forces, which are created between the tool and the workpiece that are used to grip the workpiece and feed into the SPD zone [3,4]. They are applied to deform a long billet, which is why they are called continuous processes or semi-continuous processes for SPD. Typically, these operations are realized by equal-channel angular extrusion using rolling by combining the two processes [4].

One of the most common methods of this group is ECAE - Conform [5], in which the gripping of the long billet (with active friction forces) is realized by rolling in a closed caliber between a profiled roll and a stationary die, followed by equal-channel angular extrusion.

A development of the SPD methods of this group is a new process called continuous constrained bending (a variation of the so-called "active" bending), in which the long billet is not extruded uniformly, but continuously bent through a channel with a small radius of roundness R_b, close to the height of the bent long billet T [6-9]. The process of constrained continuous double bending in calibers is realized by two profiled rolls rotating in the same direction and a bending roller between them - CCDB Conform R3D2 (or Continuous Constrained Bending Conform Rolls 3 Deformation zones 2) [10], whereby two deformation zones for SPD are realized by multidirectional bending, by realizing small relative bending radiuses $R_b/T \leq 1$ [6-10].

The aim of this work is to use CAD/CAE software 3D simulation to analyze the distribution and magnitude of effective strains in the CCDB Conform R3D2 process with small relative bending radiuses, deriving an analytical expression to determine the accumulated effective strains. For this purpose, 3D virtual tools, created in the QForm VX 8.2.4 environment, were used on the three possible options for positioning the bending roller relative to the roll axis line.

2. Materials and methods

The continuous constrained bending results in the consistent formation of two SPD zones corresponding to continuous bending and subsequent straightening of the long billet. There are three possible design solutions of CCDB Conform R3D2, according to the arrangement of the bending roller, relative to the axis of the feeding and output rolls, which are considered and analyzed, namely: - two rolls (Ø170 mm) and a bending roller with a tooth, located on a common line (Fig. 1); - two rolls (Ø150 mm) and a bending roller with a trapezoidal groove, with an axis located above (Fig. 2) and below (Fig. 3) the roll axis line.

The realization of several passes for the accumulation of these deformations in a cyclic repetition of the operation is possible, since the input size of the billet is 8 x 10 mm and in the output - 10 x 8 mm. Despite the compression in the grooves during rolling, the CCDB Conform R3D2 operation can be repeated since the dimensional values of the workpiece are not changed and its cross section is only "rotated" to 90°. The simulations were performed with billet of deformable copper alloy and the used lubricant in the die is zinc stearate.

The sample mean values for the effective strains ϵ_{CCDB} are determined in the selected cross-section according to the expression

$$\epsilon_{CCDB} = \frac{1}{n}\sum_{i=1}^{n}\epsilon_i. \quad (1)$$

where: n - the number of nodes in the cross section (n= 49); ϵ_i- the magnitude of effective plastic strain at certain nodes.

2.1 Virtual tools for continuous constrained double bending design solutions

The strain rate distribution in the two bending zones under constrained bending in a caliber (CCDB Conform R3D2 upper) with two rolls and a bending roller with a trapezoidal groove at an axis located above the roll line is given in Fig. 1.

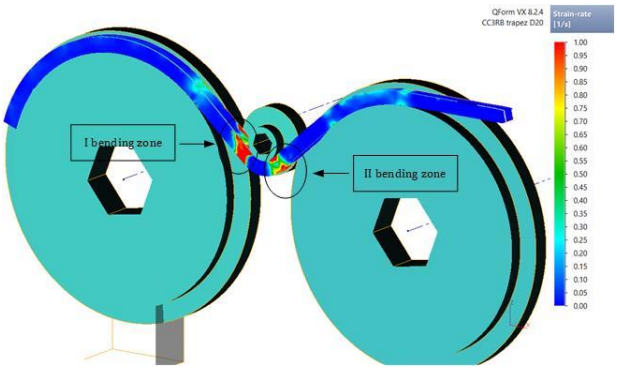

Fig. 1. Virtual tool for realizing CCDB Conform R3D2 upper with a bending roller above the axis line of the rolls (QForm VX 8.2.4).

The deformation process for constrained continuous double bending with two rolls and a bending roller with the axis located above the rolls line at $R_b/T \leq 1$ at a bending angle of 85°-95° is simulated for a roller with a diameter of 20 mm to 12 mm (Table 1).

Table 1. Sample mean values of effective strains within the virtual tool for realizing CCDB Conform R3D2 with a bending roller above the axis line.

Relative bending radius	Effective strains ϵ_{CCDB} in **CCDB Conform R3D2 upper** with a bending roller above the axis line of the rolls				
	I SPD zone	% in I zone	II SPD zone	% in II zone	Total ϵ_{CCDB}
$R_b/T = 1.1$	0.38	67	0.19	33	0.57
$R_b/T = 1.0$	0.42	66	0.22	34	0.64
$R_b/T = 0.7$	0.60	65	0.32	35	0.92

The determined total average values for the effective strains achieved only in the two deformation zones (bending/straightening) are ϵ_{CCDB} = 0.57÷0.92 (Table 1), with a distribution of about 2:1 for I SPD zone to II SPD zone, respectively.

The strain rate distribution in the two bending zones under constrained bending in calibers (CCDB Conform R3D2 center) with two rolls and a bending roller with a tooth on the line of the rolls is simulated for a roller with a diameter of 20 mm to 50 mm is given in Fig. 2.

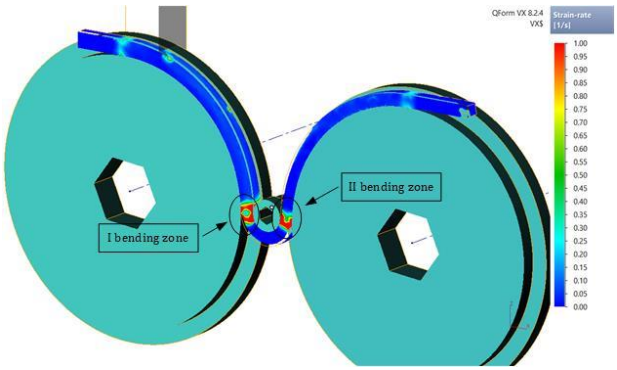

Fig. 2. Virtual tool for realizing CCDB Conform R3D2 centre with a bending roller on a common line between axes of the rolls (QForm VX 8.2.4).

The determined total mean values for the effective strains achieved only in the two deformation zones (bending/straightening) are ϵ_{CCDB} = 0.23÷0.56 (Table 2), with a distribution of about 3:2 for I SPD zone to II SPD zone, respectively (Fig. 4). The values of the relative bending radius, however, are in the range R_b/T= 1.1÷2.8, which explains the lower values of the accumulated effective strains.

The strain rate distribution in the two bending zones under constrained bending in calibers (CCDB Conform R3D2 lower) with two rolls and a bending roller with a trapezoidal groove at an axis located below the roll line is given in Fig. 3.

Table 2. Sample mean values of effective strains within the virtual tool for realizing CCDB Conform R3D2 centre with a bending roller on a common line between axes of the rolls.

Relative bending radius	Effective strains ϵ_{CCDB} in **CCDB Conform R3D2 centre** with a bending roller on a common line with the rolls				
	I SPD zone	% in I zone	II SPD zone	% in II zone	Total ϵ_{CCDB}
$R_b/T = 2.8$	0.15	65	0.08	35	0.23
$R_b/T = 1.7$	0.25	61	0.16	39	0.41
$R_b/T = 1.1$	0.32	57	0.24	43	0.56

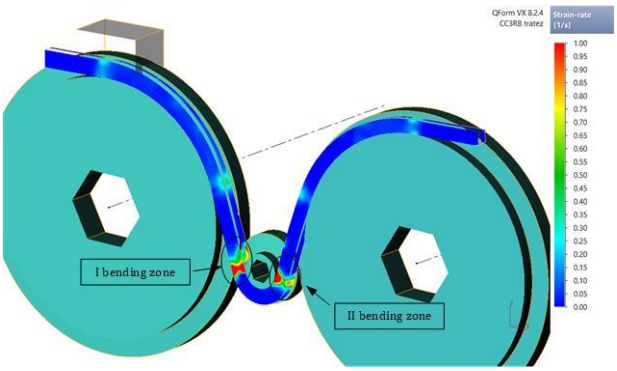

Fig. 3. Virtual tool for realizing CCDB Conform R3D2 lower with a bending roller below the axis line of the rolls (QForm VX 8.2.4).

The deformation process for constrained continuous bending with two rolls and a bending roller with the axis located below the roll line at $R_b/T \leq 1$ at a bending angle of 35^0 - 45^0 is simulated for a roller with a diameter of 20 мм to 12 мм (Table 3).

Table 3. Sample mean values of effective strains within the virtual tool for realizing CCDB Conform R3D2 lower with a bending roller below the axis line.

Relative bending radius	Effective strains ϵ_{CCDB} in **CCDB Conform R3D2 lower** with a bending roller below the axis line of the rolls				
	I SPD zone	% in I zone	II SPD zone	% in II zone	Total ϵ_{CCDB}
$R_b/T = 1.1$	0.34	63	0.20	37	0.54
$R_b/T = 0.9$	0.36	61	0.23	39	0.59
$R_b/T = 0.7$	0.40	61	0.26	39	0.66

The determined total mean values for the effective strains achieved only in the two deformation zones (bending/straightening) are ϵ_{CCDB} = 0.54÷0.66 (Table 3), with a distribution of about 3:2 for I SPD zone to II SPD zone, respectively (Fig. 4).

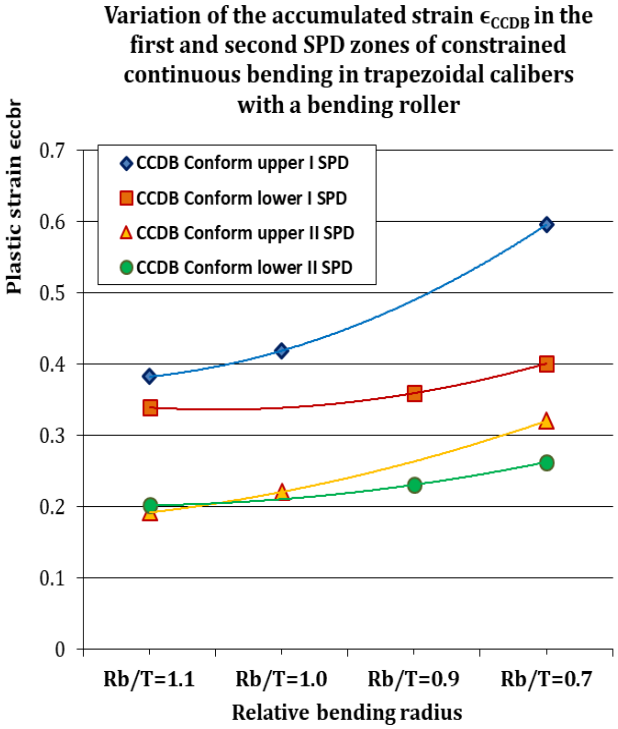

Fig. 4. Comparison of the variation of effective strains in both SPD zones under continuous constrained bending in trapezoidal calibers at small relative bending radiuses.

When comparing the values obtained for the effective strains in all three design solutions for CCDB Conform R3D2, can be seen that, similar to the "free" bending, the magnitude of ϵ_{CCDB} does not depend on the bending angle but is mainly determined by the relative bending radius R_b/T (Table 1, 2 and 3).

The variation of the total mean values of effective strains ϵ_{CCDB} under continuous constrained double bending in trapezoidal calibers for several values of the relative bending radius $R_b/T \leq 1$ is presented in Fig. 4.

Therefore, before deriving an expression for the analytical determination of the effective strains, an analysis and comparison of the new SPD process called constrained continuous bending with the classical and well-studied process - die-bending, must be performed.

2.2 Comparison between single-angle bending and continuous constrained double bending deformation zones

The comparison of the bending processes was carried out in terms of the mean stress σ_{med} and the type and distribution of the deformation zones formed by the maximum strain rate values $\bar{\epsilon}_{int}$.

Only one deformation region of contraction and elongation separated by a neutral line is observed in the "free" die-bending before compression (Fig. 5a). Similar is the distribution of the mean stress. After the combination of bending with compression in the final calibration stage of the bent blank in the die, although there is no significant change in the mean stress distribution σmed, however, two deformation zones are now clearly formed, completely separated from each other (Fig. 5b).

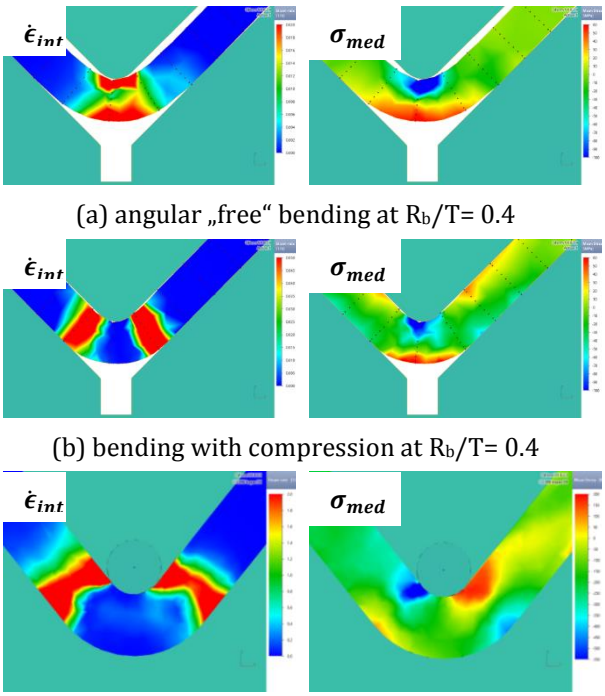

(a) angular „free" bending at R_b/T= 0.4

(b) bending with compression at R_b/T= 0.4

(c) constrained double bending at R_b/T= 0.4

Fig. 5. Variation of strain rate $\bar{\epsilon}_{int}$ (left column) and mean stress distribution σ_{med} (right column) in die-bending and continuous constrained double bending.

Compared to bending with compression, continuous constrained double bending has a development in terms of deformation zones (Fig. 5c) as they are two orders of magnitude higher in strain rates, suggesting the presence of localized severe plastic deformation. The mean stress distribution in continuous constrained bending

(Fig. 5c) is now different, being shaped into two separate mean compression/tension stress zones with a neutral line between them.

When comparing the efficiency of SPD processes, it is accepted to use not the mean stress σ_{med} itself, but its comparison with the effective stress σint, by introducing the so-called workability parameter $\beta_{int\sigma}=3.\sigma_{med}/\sigma_{int}$ [11].

The variation of the workability parameter $\beta_{int\sigma}$ in the deformation zones along the cross-section height of the deformed billet, determined from the maximum values of strain rate $\bar{\epsilon}_{int}$, for the analyzed bending processes is presented in Fig. 6. The die-bending process is represented by dotted curves in Fig. 6 (one for the "free" bending and two for the bending with compression).

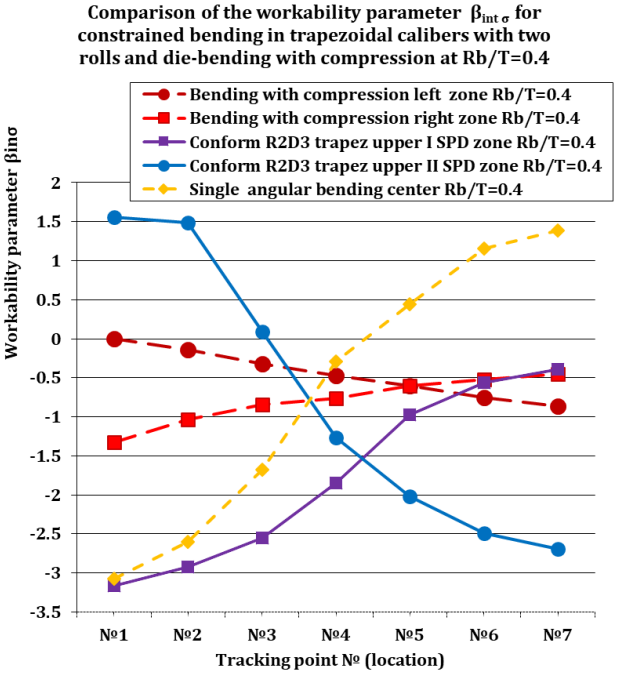

Fig. 6. Comparison of the variation of the workability parameter $\beta_{int\sigma}$ under continuous constrained bending and die-bending at relative bending radius R_b/T= 0.4

In "free" bending, the variation of the workability parameter $\beta_{int\sigma}$ is represented by only one curve, which in the flattening combination stage is transformed/unfolded into two curves, but only with negative values (all indicated by dashed curves in Fig. 6) and an intercept at $\beta_{int\sigma}\approx$ -0.5. The variation of the $\beta_{int\sigma}$ for the continuous constrained double bending has the two deformation zones formed and has a similar arrangement of curves (indicated by solid lines in Fig. 6), but with a much more negative workability parameter, which in the first deformation zone has entirely negative values ($\beta_{int\sigma}\approx$ -0.5), and the point of intersection between them is much lower - at $\beta_{int\sigma}\approx$ -1.5.

Comparison of the mean stress σ_{med}, strain rate $\bar{\epsilon}_{int}$ and variation of the workability parameter βintσ within the deformation zones suggests that the "free" bending deformation zone below the punch has been transformed into the first SPD zone in continuous constrained double bending, and the second SPD zone actually mirrors the constrained "straightening" in position of the bent long billet. This shows that the process CCDB Conform, although capable of realizing much larger strains, can use the die-bending approach for analytical determination of maximum bending strains ϵ_{bend}, which uses the geometric dimensions of the deformation space (bending radius R_b and blank height T).

2.3 Analytical determination of effective strains in CCDB conform process

The variation of the magnitude of the mean effective strains under continuous constrained double bending in calibers (Table 1, 2 and 3), shows that they are determined by the magnitude of the relative radius R_b/T rather than the bending angle, which resembles the typical relationship for single "free" bending of narrow strips, between the maximum effective strains ϵbend in the tension zone. In the case of "free" bending and a location of the neutral layer in the middle (i.e. at a distance of ½T from the inside of the deflection), the maximum effective strain in the tension zone ϵ_{bend} is given by the expression [3]:

$$\epsilon_{bend} = ln\left[1 + 1/\left(2\,{}^{R_b}/_{T} + 1\right)\right]. \qquad (2)$$

where: T - height (thickness) of the bent billet; R_b - internal bending (punch) radius.

The presence of two deformation zones (bending/straightening) and the analogy between the deformation zones in these two processes (Fig. 4) leads to the derivation of a simple relationship by doubling the engineering strains ε_{bend}, viz:

$$\epsilon_{CCDB} = ln\left[1 + 2/\left(2\,{}^{R_b}/_{T} + 1\right)\right]. \qquad (3)$$

So that the magnitude of the total mean strains in continuously constrained double bending ϵ_{CCDB}

(without taking into account the compaction of the workpiece into the grooves of the feeding/output rolls) corresponds to the doubled maximum strain in "free" bending ϵ_{bend}.

Although they are close to the total values obtained from simulation modelling, the effective strains ϵ_{CCDB} determined in this simple way do not take into account the type of conceptual solution of CCDB Conform R3D2 and especially the difference between the realised strains in the two SPD zones. The discrepancies between the effective strains determined analytically in this way (3) and the values calculated by simulation modelling (Table 1, 2 and 3) ranges from 8% for CCDB Conform R3D2 lower to 37% for CCDB Conform R3D2 upper.

2.4 Analytical determination of effective strains in CCDB conform SPD zones

In order to distribute more accurately the accumulated strains in the two SPD zones, it is necessary, instead of doubling, to add a new virtual constrained bending coefficient k_{bi} when determining the effective strains, whereby the expression (3) takes the form:

$$\epsilon_{CCDB} = ln\left[1 + k_{bi}/\left(2\,{}^{R_b}/_{T} + 1\right)\right]. \qquad (4)$$

This allows the continuously constrained double bending process to be divided and the effective strains in two separate SPD zones to be determined. The dependence (4) does not contradict, but is in fact a development of expression (3) at a virtual continuously constrained bending coefficient k_b= 2.
Comparing the values of k_{b1} and k_{b2} obtained according to expression (4) and according to expression (3) the effective strains ϵ_{CCDB} for the first and second SPD zones of CCDB Conform R3D2 with bending roller above the rolls line are given in Table 4.

Calculated according to expression (4), the virtual active bending coefficient k_{b1} in I SPD zone ranges from 1.5 to 1.9, and k_{b2} in II SPD zone ranges from 0.7 to 0.9, demonstrating the sensitive difference between these two deformation zones. The difference between the analytically determined total effective strain ϵ_{CCDB} according to (3) and the values calculated by simulation modeling at k_b= 2 (Table 1) is from 19% to 48%.

Table 4. Sample mean values of effective strains within the virtual tool for realizing CCDB Conform R3D2 with a bending roller above the axis line.

Relative bending radius	Determined strains ϵ_{CCDB} (4) in CCDB **Conform R3D2 upper** with a bending roller above the axis line of the rolls				
	I SPD zone	k_{b1}	II SPD zone	% in II zone	ϵ_{CCDB} (k_b=2)
R_b/T = 1.1	0.382	1.50	0.191	0.68	0.483
R_b/T = 1.0	0.419	1.56	0.220	0.74	0.511
R_b/T = 0.7	0.596	1.90	0.320	0.88	0.619

The comparison of the values of kb1 and kb2 obtained according to expression (4) and according to expression (3) effective strains ϵ_{CCDB} for the first and second SPD zones of CCDB Conform R3D2 with bending roller below the rolls line are given in Table 5.

The virtual active bending coefficient k_{b1} calculated according to expression (4) in I SPD zone is from 1.2 to 1.3 and k_{b2} in II SPD zone is 0.7. The difference between the analytically determined total effective strain ϵCCDB according to (3) and the values calculated by simulation at k_b= 2 (Table 3) is 7% to 12%.

Table 5. Sample mean values of effective strains within the virtual tool for realizing CCDB Conform R3D2 with a bending roller below the axis line.

Relative bending radius	Determined strains ϵ_{CCDB} (4) in CCDB **Conform R3D2 lower** with a bending roller lelow the axis line of the rolls				
	I SPD zone	k_{b1}	II SPD zone	% in II zone	ϵ_{CCDB} (k_b=2)
R_b/T = 1.1	0.339	1.30	0.202	37	0.72
R_b/T = 1.0	0.359	1.20	0.230	39	0.72
R_b/T = 0.7	0.401	1.15	0.262	39	0.70

The comparison of the variation of the virtual coefficients of continuously constrained bending in trapezoidal calibers k_{b1} and k_{b2}, depending on the variation of the relative bending radius $R_b/T \leq 1$ is presented in Fig. 7. It can be seen that the values of the coefficients $k_{b1} > 1$ и $k_{b2} < 1$ increase with decreasing relative radius R_b/T, which follows the trend of the variation of the corresponding effective strains ϵ_{CCDB} (Fig. 4).

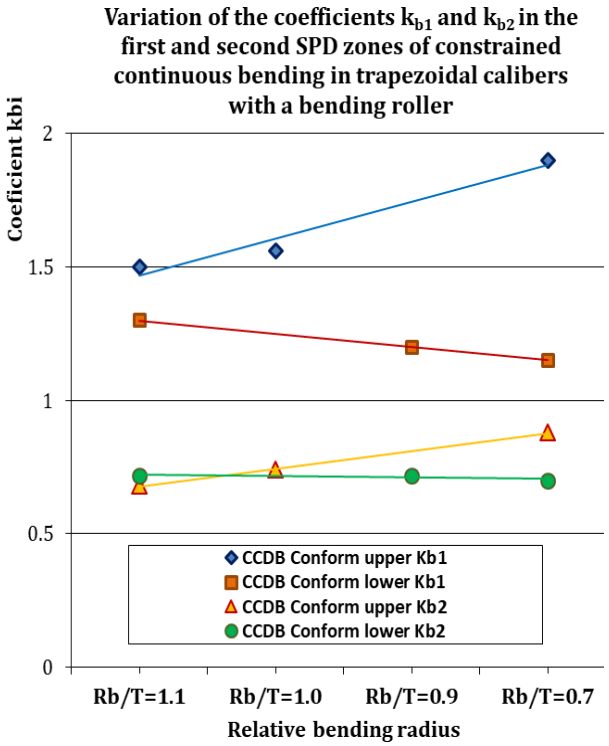

Figure 7. Comparison of the variation of the virtual active bending coefficient under CCDB Conform R3D2 at small relative bending radiuses $R_b/T \leq 1$.

The comparison of the values of k_{b1} and k_{b2}, obtained according to expression (4) and according to expression (3) effective strains ϵ_{CCDB} for the first and second SPD zones of the CCDB Conform R3D2 with bending roller on the line between the rolls are given in Table 6.

The virtual active bending coefficient k_{b1} calculated according to expression (4) in I SPD zone is from 1.1 to 1.2 and k_{b2} in II SPD zone is from 0.6 to 0.9. The difference between the analytically determined total effective strain ϵ_{CCDB} according to (3) and the values calculated by simulation modelling at $k_b = 2$ (Table 6) is from -13% to 17%.

Table 6. Sample mean values of effective strains within the virtual tool for realizing CCDB Conform R3D2 with a bending roller below the axis line.

Relative bending radius	Determined strains ϵ_{CCDB} (4) in CCDB **Conform R3D2 centre** with a bending roller on a common line with the rolls				
	I SPD zone	k_{b1}	II SPD zone	% in II zone	ϵ_{CCDB} (k_b=2)
R_b/T = 2.8	0.150	1.06	0.082	0.56	0.266
R_b/T = 1.7	0.250	1.23	0.162	0.76	0.379
R_b/T = 1.1	0.321	1.22	0.241	0.88	0.483

When comparing the values obtained for the virtual active bending coefficients for all three constructive solutions, it can be seen that the magnitude of virtual continuously constrained bending coefficients $k_{b1} > 1$ and $k_{b2} < 1$ depends mainly on the deformation zone and the positioning of the bending roller, increasing relatively little as the relative bending radius decreases (Fig. 7).

3. CONCLUSION

1. The three constructive solutions of the continuously constrained double bending with active friction forces at small relative bending radiuses are considered and analyzed in terms of the accumulated mean values of effective strains within the virtual tools for realizing CCDB Conform R3D2 process.
2. The continuously constrained double bending and die-bending processes are compared in terms of the variation of the workability parameter β_{into} and strain rate $\bar{\epsilon}_{int}$ within the deformation zones formed by the simulation modelling.
3. It is found that the magnitude of the total mean strains in continuously constrained double bending ϵ_{CCDB} corresponds to the doubled maximum strain in "free" bending ϵ_{bend} and a simple general relationship for its analytical determination is proposed.
4. The relation for the analytical determination of the effective strains in the two SPD zones of CCDB Conform R3D2 of the form $\epsilon_{CCDB} = ln\left[1 + k_{bi}/\left(2\,{}^{R_b}/_{T} + 1\right)\right]$ is suggested, and the variation of the virtual continuously constrained bending coefficients $k_{b1} > 1$ and $k_{b2} < 1$ is determined, depending on the process, the type of zone and the variation of the relative bending radius R_b/T.

Acknowledgement

This work was supported by the European Regional Development Fund within the Operational Programme "Science and Education for Smart Growth 2014 - 2020" under the Project CoE "National center of mechatronics and clean technologies" BG05M2OP001-1.001-0008.

REFERENCES

[1] G. Faraji, H. S. Kim, and H. T. Kashi, Severe plastic deformation: Methods, Processing and Properties. Elsevier, 2018.

[2] A. Rosochowski: *Severe Plastic deformation Technology*, Whittles Publishing, 2017.

[3] J. Genov, V. Kamburov, "Processing of metals by plastic deformation," *MP TU-Sofia*, p. 151. 2019.

[4] V. Kamburov, "Theoretical aspects and virtual solutions for severe plastic deformation with reduced and active friction forces," *Copy Print Studio*, p. 220. 2021.

[5] D. Green, "Continuous Extrusion-Forming of Wire Section," *Jornal of the Institute of Metals*, vol. 100, pp. 295-300, 1972.

[6] G.J. Raab, R.Z. Valiev, T.C. Lowe, Y.T. Zhu, "Continuous processing of ultrafine grained Al by ECAP–Conform," *Materials Science and Engineering: A*, vol. 382, no. 1–2, pp. 30–34, Sep. 2004, doi: 10.1016/j.msea.2004.04.021.

[7] V. Kamburov, "Continuous Constrained 3 rolls Bending with active friction forces based on double Conform process," *2019 II International Conference on High Technology for SustainableDevelopment(HiTech)*,Oct.2019.doi.org/10.1109/HiTech48507.2019.9128273.

[8] V. Kamburov, "Constrained Continuous Bending in Trapezoidal Calibers with Three Grooved Rolls," *2021 IV International Conference on High Technology for Sustainable Development (HiTech)*, Oct. 2021. doi.org/10.1109/HiTech53072.2021.9614227.

[9] V. Kamburov, A. Nikolov, "Comparison of the Continuous Constrained Double Bending process with Equal Channel Angular Extrusion Conform process by simulation modelling," *Proceedings of 13th National Conference Electronica*, May 2021.

[10] V. Kamburov, J. Genov, A. Yordanov, A. Nikolov, R. Dimitrova, Y. Sofronov, "Device for limited continuous two-stage bending," Utility model Patent №4262, 02.02.2022.

[11] V. Vujovic and A. H. Shabaik, "A new workability criterion for ductile metals," *Journal of Engineering Materials and Technology-transactions of the Asme*, vol. 108, no. 3, pp. 245–249, Jul. 1986, doi: 10.1115/1.3225876.